COUPLING HYPERSPECTRAL REMOTE SENSING WITH FIELDSPECTROMETER TO MONITOR INLAND WATER QUALITY PARAMETERS

Naseer A. Shafique,[1] Florence Fulk[2] and Susan M. Cormier,[2] Bradley C. Autrey[1]

INTRODUCTION

Stream ecosystems around the world are being impacted by eutrophication. Eutrophication is the state of having high nutrient content and high organic production (Wetzel, 1995). It diminishes water quality by promoting the excessive growth of algae, cyanobacteria (blue-green algae) and macrophytes. Environmental researchers have been making efforts to monitor, simulate and control eutrophication for more than two decades. Various mathematical models have been developed and applied to rivers, lakes and estuaries (Lung, 1986; Thomann and Mueller, 1987; Kuo and Wu, 1991; Kuo et al., 1994). Most water quality models simulate increases in eutrophication based on initial conditions of the water body, therefore, demanding comprehensive water quality sampling programs. However, the conventional measurement of water quality requires in situ sampling and expensive and time-consuming laboratory work. Due to these limitations, the sample size often cannot be large enough to cover the entire water body. Therefore, the difficulty of synoptic and successive water quality sampling becomes a barrier to water quality monitoring and forecasting.

Remote sensing could overcome these constraints by providing an alternative means of water quality monitoring over a range of temporal and spatial scales. A number of studies have shown that applications of remote sensing can meet the demand for the large sample sizes required of water quality studies conducted on the watershed scale. Imagery from satellite and aircraft remote sensing systems have been used in the assessment of water quality parameters such as temperature, chlorophyll *a*, turbidity, and total suspended solids (TSS) for lakes and reservoirs (Lillesand et al., 1983; Lathrop and Lillesand, 1989; Ritchie and Cooper, 1991), estuaries (Verdin, 1985; Harding et al., 1995) and tropical coastal areas (Ruiz-Azuara, 1995).

Previous studies have focused on the discovery of the relationship between remote sensing data and in-situ measurements. To make remote sensing tools useful for practical applications, water quality modeling must be incorporated with water quality monitoring programs. Moreover, integrating a geographic information system (GIS) allows for the display of refined monitoring simulation results, rather than the use of traditional numerical figures. This provides a means by which water quality modeling data can be presented in a way that is practical for water quality management. The specific objectives of this study were to: 1) establish a model to process remote sensing data and provide a rapid and efficient water quality monitoring technique for a wide area, 2) present predicted water quality conditions temporally and spatially on a georeferenced map and 3) display sequential (temporal) images of water quality predictions to provide decision makers with easily understandable information.

Study Area

The study site is located in southwest Ohio and includes the Great Miami River (a tributary of the Ohio river), as well as adjacent water bodies, including fishponds, reservoirs and other rivers that are tributaries of the Ohio River.

The Great Miami River is situated in the Miami basin, which encompasses the drainage basins of both the Little and Great Miami Rivers (Figures 1 and 2). The Miami basin includes most of southwestern Ohio and portions of Indiana. The major waterways are the Great Miami River (including the tributaries, the Stillwater and Mad Rivers), the Little Miami River, and Whitewater River in Indiana.

Landforms in the Great Miami River Watershed have been shaped by glaciations, which left flat-to-gently-rolling terrain, glacial till, and in some areas, exposed limestone and shale. Soils in the watershed tend to be neutral-to-slightly alkaline and drainage varies from well drained to very poorly drained, depending on parent material and topography. The river lies within a broad valley with a wide flood plain (Ohio EPA, 1997). The area drained by the

[1] SoBran Environmental Inc: Shafique.Naseer@epa.gov
[2] US Environmental Protection Agency: Fulk.Florence@epa.gov

major waterways includes both agricultural and urban lands (Ohio EPA, 1997). The Miami basin includes the major cities of Cincinnati and Dayton, Ohio, and the smaller cities of Hamilton and Middletown, Ohio along the Great Miami River. Currently, it is estimated that 70% of the total land area is used for agriculture, dominated by row crops of corn and soybeans. Urban areas occupy 13% of the land, forested areas occupying 7%, and wetlands and water bodies occupy 1% of the total land area in the Miami basin (USGS, unpublished report).

The Ohio Environmental Protection Agency (Ohio EPA) noted that most industries and municipalities near the Great Miami River utilize groundwater as a principal water source but discharge treated wastewater to the river. Surface run off from agricultural or urban areas and industries along the river is not treated or impeded prior to entering the river (Ohio EPA, 1997).

Both the U.S. Environmental Protection Agency (USEPA) and the U.S. Geological Survey (USGS) have identified six important water quality issues in the Miami basin. These include: 1) the degradation of surface-and ground-water quality by urban and agricultural sources of fertilizer and pesticides, 2) assessing the relative importance of point and non-point sources to contaminant loads in the Great and Little Miami River basins, 3) habitat degradation and decreases in stream biodiversity as a result of urbanization, 4) the occurrence of water-borne pathogens in streams and shallow ground water in rural and urban land-use settings, 5) the effect of septic systems and combined sewer overflows on surface and shallow ground-water quality, and 6) the disruption and fragmentation of stream habitats by low dams and impoundments and their effects on fish and benthic invertebrate communities (Ohio EPA, 1997).

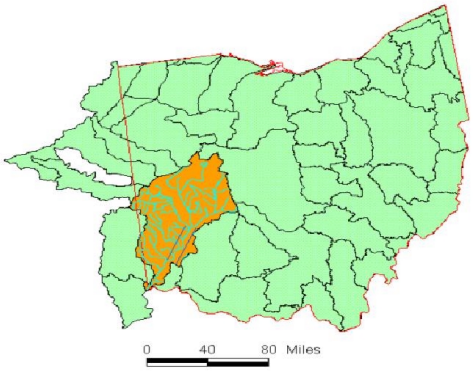

Figure 1: Location map.

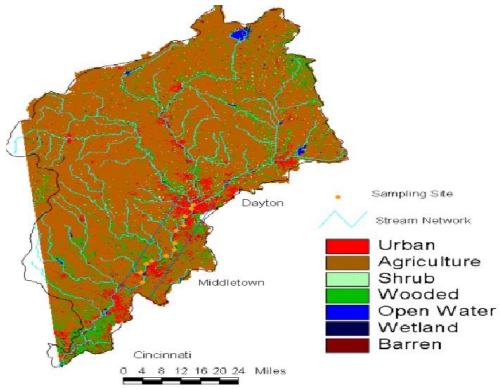

Figure 2: Sampling site of the Great Miami River within the Miami River basin.

The presence of these environmental concerns in the Miami basin and the availability of ancillary data in the offices of the USEPA, OEPA, Ohio Department of Natural Resources (ODNR), Natural Resources Conservation Commission (NRCS) and USGS make the Miami basin an appropriate pilot study site for this type of research. A map of the study locations within the Miami basin is shown in Figure 2.

DATA

Ground truth (reference) and spectral data were collected from 26 January 1999 to 30 September 1999. The data can be roughly divided into two sets, preliminary and pilot, based on the date and location from which the data were collected and the amount of data collected. The preliminary data sets were collected from 26 January 1999 to 12 April 1999 and the pilot data sets were collected from 14 May 1999 to 30 September 1999. In addition, all pilot data were collected from the Great Miami River between river miles (RM) 45 and 92, where remote sensing imagery was acquired in the latter part of the study period. The purpose of the preliminary data was to examine the response of the Full Range Field Spectroradiometer (FieldSpec FR, Range 350-2,500 nm) to different water quality conditions found in the various water bodies. Generally, the preliminary spectral reading was accompanied by turbidity measurements using a field turbidimeter. In addition, in-vivo chlorophyll measurements were made on two additional dates. The other major data set for this project includes two sets of hyperspectral imagery. The airborne sensor that acquired the imagery was the Compact Airborne Spectrometer Imager (CASI), taken on 8 and 9 September 1999. The CASI acquired imagery in 19 spectral bands and the HyMap acquired imagery in 126 spectral bands.

Spectral Data Collection

Two types of spectral data were collected during the study period: above water reflectance spectra and underwater radiance or irradiance spectra. The reflectance data represent the ratio of reflected energy to incident energy with values ranging from 0.0 to 1.0. The irradiance data represent actual energy received by the sensor as downwelling (irradiance) or upwelling (radiance) in units of power per unit area per unit wavelength ($W/m^2/sr/nm$). The above water reflectance data were collected using the FieldSpec FR instrument from Analytical Spectra Devices (ASD), Inc., 1999. The underwater radiance spectra were collected using two methods. The first method used the FieldSpec FR instrument fitted with an underwater extension cord and an Underwater Remote Cosine Receptor (UWRCR). The second method used a Li-Cor brand light meter (LI-189) with an underwater sensor (LI-1000). While the FieldSpec FR samples energy (reflected or radiant) at 1-nm intervals, the Li-Cor measured an aggregate energy in the visible range between 400 and 700 nm. Due to the amount of time it takes to assemble and disassemble the underwater extension to the FieldSpec FR, the underwater extension was used only during the first day of the CASI flyover. Thus, the instrument of choice for most underwater light measurement was the Li-Cor meter. An apparatus was constructed to position the sensors at the desired depth, pointing upward to measure downwelling irradiance and downward to measure upwelling radiance).

Imagery

On 8 and 9 September 1999, Hyperspectral Data International (HDI) flew the CASI sensor over the Great Miami River from approximately RM 45 to approximately RM 92. This sensor acquired data in 19 spectral bands with a spatial resolution of 2 m. Twenty three flightlines covered approximately 80 km (49.7 miles) of the Great Miami River, from Middletown, Ohio to the Taylorsville Dam, approximately 15 km (9.3 miles) north of Dayton, Ohio. The imagery was delivered on 36 compact discs (CDs) in a band sequential (BSQ) file format that was imported with the Environment for Visualizing Images (ENVI) processing software. Some of the flight lines were split into several segments for the purpose of pre-processing (Hyperspectral Data International, 2000). Data obtained with the hand-held spectroradiometer were analyzed, revealing seven spectral bands that demonstrated usefulness for water quality studies. These include, bands 2 (440 nm), 7 (625 nm), 11 (672 nm), 14 (705 nm), 16 (740 nm), 17 (816 nm) and 18 (840 nm). These are the minimum number of bands that could be used to develop preliminary water quality maps.

METHODS

Criteria of Band Selection

Absorption

Through the components of light absorption and scattering coefficients, the water body controls the ratio between light scattering and absorption values, and thus determines the subsurface reflectance and in turn the emergent flux that will be sensed by radiometers (Jupp et al., 1994). Because the medium composition affects the absorption and scattering coefficients differently at various wavelengths, the resulting spectral distribution can be mathematically modeled and/or measured by a spectroradiometer from above and under the water's surface, and thus can be used to provide information about the water body.

Both field and laboratory spectrometric measurements of reflectance and absorbance are essential to developing semi-empirical and analytical (radiative transfer) models that can describe the interactions of light and in-water materials (Dekker, 1997). Field spectrometry is the quantitative measurement of radiance, irradiance, reflectance or transmission of light in the field. There are many reasons why it is desirable to perform spectral measurement in the field. Field spectra of ground and water targets that are homogeneous at the scale of the imaging sensor and collected using ambient solar illumination can be used to convert radiance images to reflectance (Conel et al., 1987a,b). Often, field spectra of target materials are collected to allow for more precise image analysis and interpretation (Goetz and Srivastava, 1985). Hand-held spectroscopy is also used as a tool to perform feasibility studies to understand if and how a process or material of interest can be detected using remote sensing. Field spectra of both the material(s) of interest and spectra of other materials present in the environment can be used to address such issues as what spatial and spectral resolutions are required for detection. Lab spectroscopy measurements are also desirable because they are used for the determination of the inherent optical properties of water by measuring the absorption and scattering spectra of dissolved materials and particulate matter.

Correlation

The correlation between temporally pooled groundtruth and spectral data was used to locate spectral signatures for water quality parameters. Replicate groundtruth data at a sampling point were averaged before conducting the correlation. Thus, when available, a data point represented the mean of three replicates. There were two spectral samples, taken a few seconds apart, for each sampling point. These values were averaged before calculating the correlation with the groundtruth data. A statistical summary of all groundtruth data was first computed using descriptive statistical parameters (e.g., mean, maximum value, minimum value). This allowed the data sets to be examined for the detection of the extreme outliers.

One of the tools used to quantify the relationship between the spectral data and the groundtruth data was a correlation matrix. Scatter plots of groundtruth data against spectral data and of groundtruth parameters of interest against each other were made to investigate relationship trends that may not be captured by correlation values. Depending on the magnitude of the correlation values and the trend in the scatter plots, linear and non-linear equations were developed to predict water quality parameters from spectral indices.

First Derivative

Spectroscopic derivatives are tools that can be used in spectroscopy (Philpot, 1991). They are obtained by taking the difference between the reflectance of two bands and dividing that value by the difference between the wavelengths separating the two bands. Then, a correlation test is performed between derivative reflectance and the field measurement of turbidity. When the two bands used in the calculation are adjacent to one another, the result is the first derivative. It is assumed that the components of variation are additive constants acting in a spectrally independent way over a spectral range of a few nanometers (nm). This assumption fits well with knowledge of the behavior of radiation and reflectance in the atmosphere and water, moreover it is much less demanding than the assumption made for the use of broad waveband indices. The mathematical basis of derivative spectroscopy has been reviewed (Dixit and Ram, 1985) and applied to the remote sensing of vegetation (Curran, 1989; Demetriades-Shah et al., 1990; Curran et al., 1991).

The use of derivative spectroscopy for estimating turbidity and suspended particles is not frequently reported in the literature, however its potential can be inferred from previous studies (Dick and Miller, 1991; Philpot, 1991) and demonstrated using three laboratory spectra (Chen et al., 1991). The derivative reflectance spectra vary in a regular way with turbidity. Three regions of the spectrum at wavelengths near 450-550 nm, 675-750 nm and 800-1000 nm show particularly large changes in derivative reflectance with turbidity and these are, therefore, candidate spectral regions for the estimation of turbidity with derivative spectroscopy.

RESULTS AND DISCUSSION

The evaluation of band selection criteria leads to the selection of certain channels from the whole dataset for various water quality parameters. The bands integral to the most significant parameters, chlorophyll *a* and turbidity, are discussed below.

Chlorophyll a

Chlorophyll *a* is a phytopigment present in all algae groups in inland waters and shows distinct absorption bands in the blue wavelength range at 440 nm and in the red wavelength range from 672-678 nm (Figure 3), leaving a maximum green reflectance due to an internal cell scattering process. The red edge ascent near 705 nm that is narrowed to a peak by growing water absorption in the infrared is also correlated to increasing chlorophyll *a* contents (Figure 4).

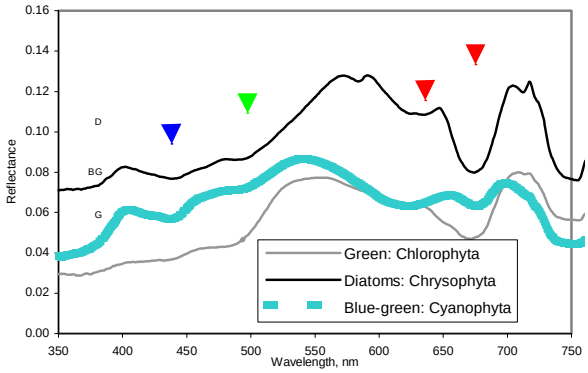

Figure 3: Absorption maxima and minima in reflectance spectra of pure algal culture.

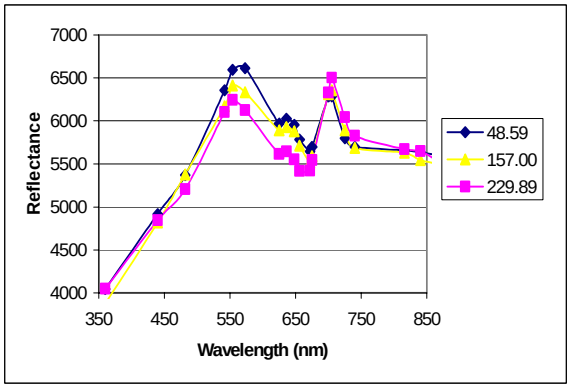

Figure 4: Reflectance spectra for known chlorophyll *a* values from CASI data.

Based on the correlation with the ground truth data, one of the most important relationships observed in this study was the relationship between turbidity, TSS, and chlorophyll. Turbidity was positively correlated with TSS (r = 0.76) and less positively correlated with chlorophyll (r = 0.37). Turbidity was negatively correlated with Secchi disk depth (r = -0.55), river depth (r = -0.19), and pH (r = -0.64). TSS was moderately correlated with chlorophyll parameters (up to r = 0.51). Of the chlorophyll parameters, turbidity and TSS generally appear to correlate better with a chlorophyll parameter that combines chlorophyll *a* and pheophytin data. Dissolved oxygen showed a low positive correlation (r = 0 to 0.49) with most parameters, but with a relatively stronger value with chlorophyll variables (r = 0.44), asserting that more living algal activity enriches the water with DO through the process of photosynthesis.

The two most significant bands, 672 nm and 705 nm, were selected for the calibration of chlorophyll *a* concentration. The ratio of 672 and 705 nm wave bands produced a good correlation (r = 0.86) with the chlorophyll *a* concentration (Figure 5). Using this linear model, a chlorophyll-a distribution map of the river was made (Figure 6). It is interesting to see that a plume of relatively clean water (lower chlorophyll-a concentration) is entering the river from the wastewater treatment plant.

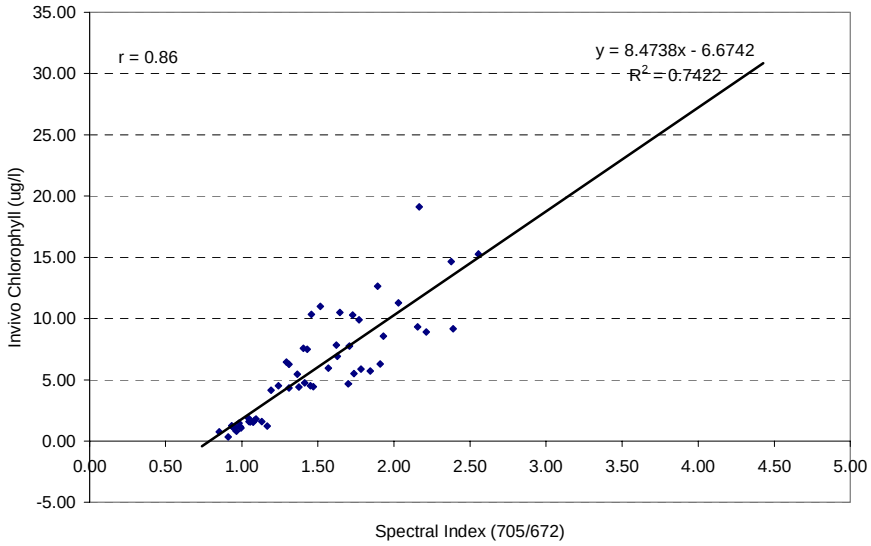

Figure 5: Correlation between spectral index and chlorophyll concentration obtained from the ground truth data.

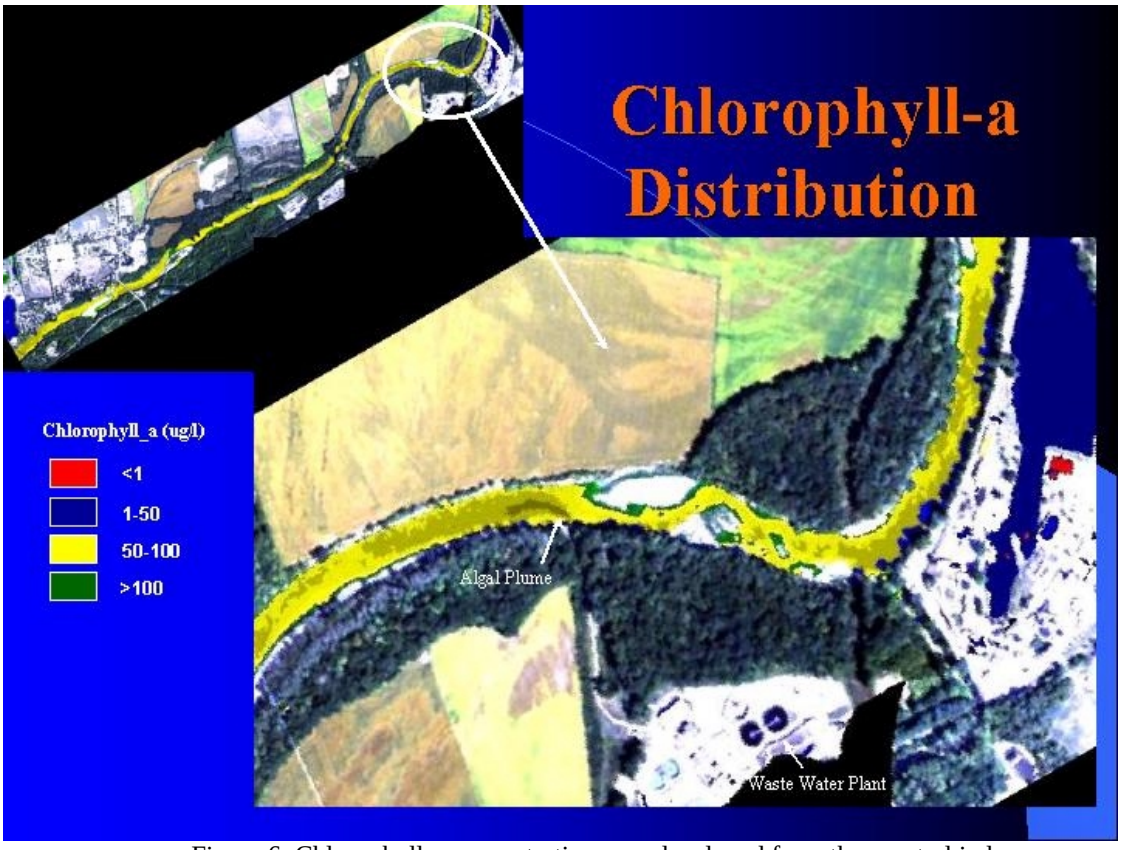

Figure 6: Chlorophyll *a* concentration map developed from the spectral index.

Turbidity

To examine the association between spectral reflectance and turbidity, correlation analyses were applied to the Fieldspec FR channels between 400 and 880 nm. A strong relationship existed between turbidity and reflectance with r = 0.8 at (625-440)*705/672. However, this relationship resulted in much higher predicted values of turbidity in the river than the turbidity values that were actually collected on the ground. In an effort to improve results, first derivatives were calculated by dividing the difference between successive reflectivity values by the wavelength interval separating them. A correlogram for turbidity was developed using the first derivative and normal reflectance at a particular wavelength. Figure 7 illustrates the difference between the correlation coefficients from the raw reflectance data and the first derivative method.

The maximum correlation, r = 0.76 was found at the derivative of (700-675)/25 nm (Figure 7). Therefore, the bands at this wavelength were selected for the turbidity measurement.
The first derivative reflectance and turbidity scatter plot (Figure 8) fits with a linear model:

Turbidity = 1224.4* (R(685)) + 3.9561 with $R^2 = 0.7917$

Using this linear model, a turbidity map of the river was made (Figure 9). This model showed a strong agreement between observed and estimated turbidity values (Figure 10).

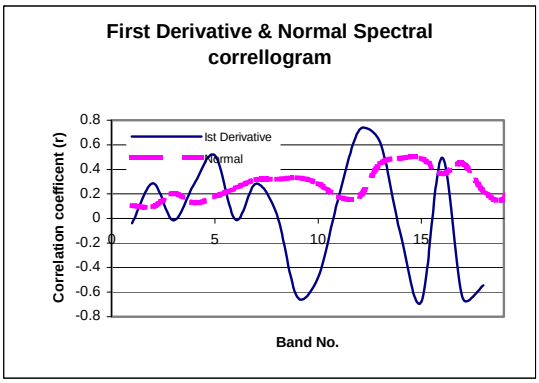

Figure 7: Comparison of first derivative and normal correlogram, higher correlation obtained from the first derivative.

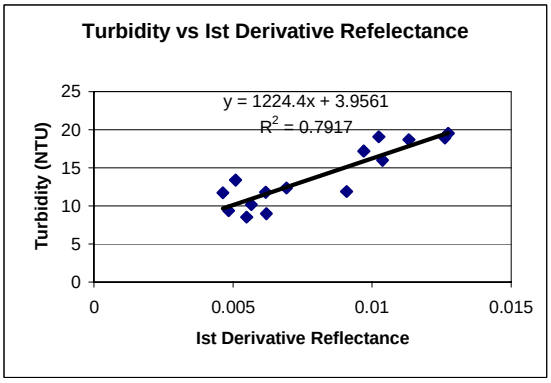

Figure 8: Correlation between first derivative reflectance and turbidity obtained from the field spectrometer data.

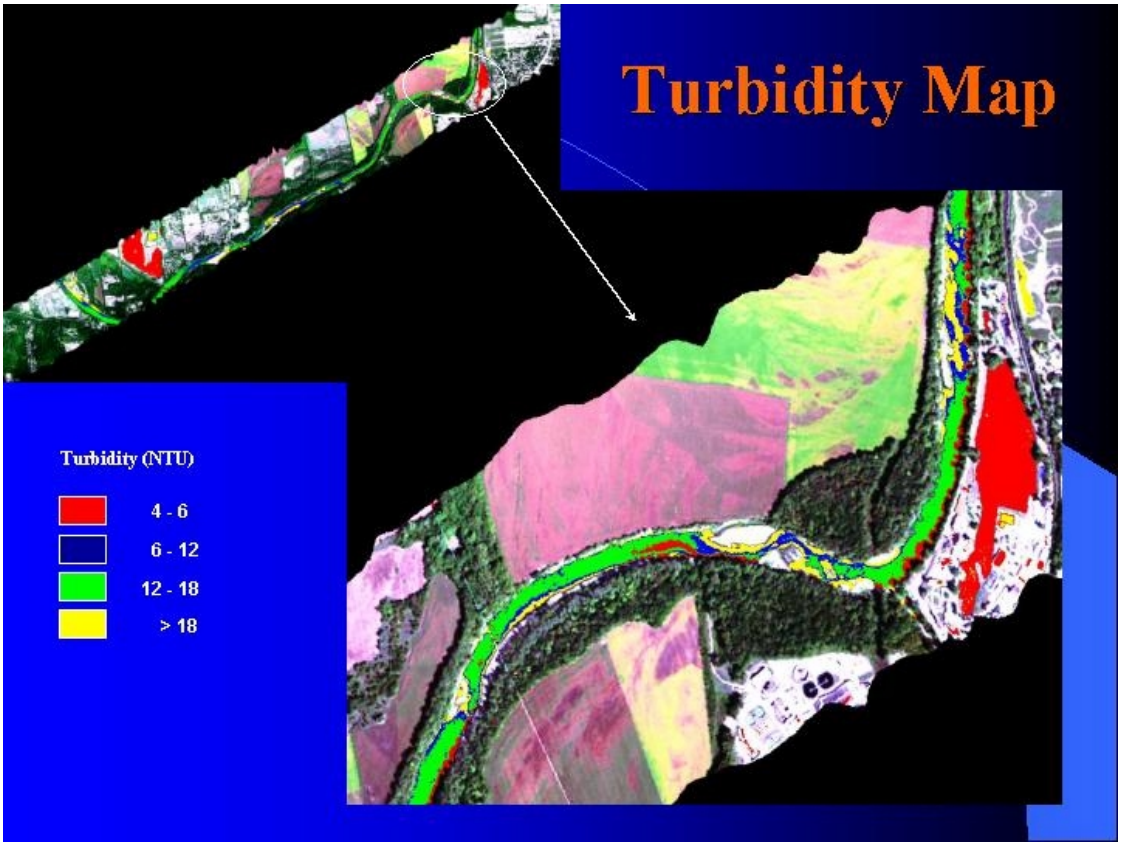

Figure 9: Turbidity distribution map of GMR, relatively clear water is entering into the river from the wastewater treatment plant.

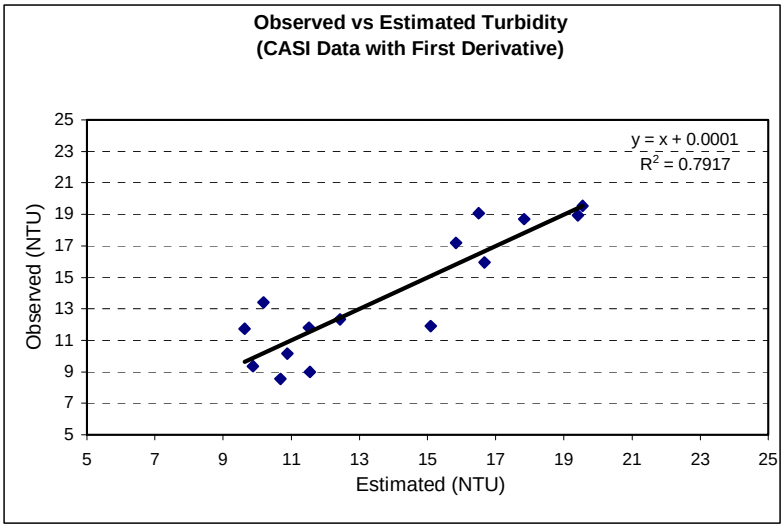

Figure 10: Observed and estimated turbidity plot, high R^2 reflects the validity of the results.

CONCLUSIONS

Remotely sensed hyperspectral data have been used successfully to map the spatial distribution of chlorophyll *a* concentrations and turbidity in the Great Miami River, Ohio. Spectral signatures from the hand-held spectrometer and airborne hyperspectral imagery showed promising correlations with ground truth water quality parameters such as algal chlorophyll concentrations, turbidity values, secchi disk depths and light extinction coefficients. Due to the presence of the strong correlation between laboratory-measured TSS and derivative reflectance with both field spectrometer data and CASI data, a first derivative spectrometry was used which showed promising results for the low-turbidity conditions of the Great Miami River. This was not possible with normal (i.e., ratio or combination) indices due to the lack of gradient in actual turbidity measurements. The imagery and the final map confirmed this uniformity in the distribution of turbidity for most of the river. Finally, maps of relative spatial distributions of chlorophyll and turbidity were created from the selected signatures derived from the imaging spectrometer data.

The hyperspectral chlorophyll and turbidity map demonstrate the spatial variability of the contents of chlorophyll and suspended matter that help determining the point and non point sources responsible for the spatial variability for the Great Miami River. As a result these maps may help to obtain more representative monitoring locations of suspended matter and related parameters as chlorophyll and secchi depth. Overall conclusion of this study was that the combined use of water quality model results, hyperspectral data and field spectrometer in situ data leads to better monitoring and understanding of suspended matter and transparency in the Great Miami River.

REFERENCES

Chen, Z., J.D. Hanson, and P.J. Curran, 1991, "The form of the relationship between suspended sediment concentration and spectral reflectance and its implications for the use of Daedalus 1268 data", *Int. J. Remote Sens,* 12:15-222.

Conel J.E., C.J. Bruegge, and B. Curtiss, 1987a, "Correcting airborne imaging spectrometer measurements for the atmosphere: A comparison of methods." Proc. 31st. S.P.I.E. International Technical Symposium on Optical and Optoelectronic Applied Science and Engineering.

Conel J.E., R.O. Green, G. Vane, C.J. Bruegge, R.E. Alley, and B. Curtiss, 1987b, "AIS-2 Radiometry and a comparison of methods for the recovery of ground reflectance." Proc. 3rd Airborne Imaging Spectrometer Data Analysis Workshop.

Curran, P.J., 1989, "Remote sensing of foliar chemistry," *Remote Sens. Environ.* 29:271-278.

Curran, P.J., J.L. Dungan, B.A. Macler, and S.E. Plumer, 1991, "The effect of a red leaf pigment on the relationship between red edge and chlorophyll concentration," *Remote Sens. Environ.* 35:69-76.

Dekker, A.G., 1997, "Operational tools for remote sensing of water quality: A prototype tool kit. Vrije Universiteit, Amsterdam Institure for Environmental Studies." BCRS Report 96-18, ISBN 90 5411 215 8.

Demetriades-Shah, T.H., M.D. Steven, and J.A. Clark, 1990, "High resolution derivative spectra in remote sensing," *Remote Sense. Environ.* 33:55-64.

Dick, K., and J. Miller, 1991, "Derivative analysis applied to high resolution optical spectra of freshwater lakes." Proc. 14th Canadian Symposium on Remote Sensing, Canadian Remote Sensing Society, Ottawa, pp. 400-418.

Dixit, L. and S. Ram, 1985, "Quantitative analysis by derivative electronic spectroscopy," *Appl. Spectrosc. Rev.* 21:311-418.

Goetz, A.F.H. and V. Srivastava, 1985, "Mineralogical mapping in the Cuprite mining district, Nevada," Proc. Airborne Imaging Spectrometer Data Analysis Workshop, April 1985, JPL Publication, no. 85-41.

Harding, L.W., E.C. Itsweire, and W.E. Esalas, 1995, "Algorithm development for recovering chlorophyll concentrations in the Chesapeake Bay using aircraft remote sensing, 1989-91," Photogrammetric *Engineering & Remote Sensing*, 61(2):177-185.

Hyperspectral Data International (HDI), Inc., 2000, "Final Report: Great Miami River Remote Sensing Project." Work Number 99RD037R. Hyperspectral Data International, Inc., Dartmouth, Nova Scotia, Canada. 57 pp.

Jupp, D.L.B., J.T.O Kirk, and G.P. Harris, 1994, "Detection, identification and mapping of cyanobacteria: Using remote sensing to measure the optical water quality of turbid inland waters, Aust. J. Mar. Freshwater Res., 45:801-828.

Kuo, J.T., J.H. Wu, and W.S. Chu, 1994, "Water quality simulation of Te-Chi Reservoir using two-dimensional models." *Wat. Sci. Tech* 30(2):63-72.

Kuo, J.T., and J.H. Wu, 1991, "A nutrient model for a lake with time-variable volumes." *Wat. Sci. Tech* 24(6): 133-139.

Lathrop, R.G., and T.M. Lillesand, 1989, "Monitoring water quality and river plume transport in Green Bay, Lake Michigan with SPOT-1 imagery." *Photogrammetric Engineering & Remote Sensing*, 55(3): 349- 354.

Lillesand, T.M., W.L. Johnson, R.L. Deuell, O.M. Lindstrom, and D.E. Meisner, 1983, "Use of Landsat data to predict the trophic state of Minnesota Lakes." *Photogrammetric Engineering & Remote Sensing*, 49(2):219-229.

Lung, W.S., 1986, "Assessing phosphorus control in the James River Basin." *Journal of Environmental Engineering*, 112(1): 44-60.

Ohio EPA, 1997, "Biological and water quality study of the Middle to Lower Great Miami River and Selected tributaries." Division of Surface Waters, Monitoring and Assessment Section, Columbus, OH. Ohio EPA Technical Report MAS/1996-12-8.

Philpot, W.D., 1991, "The derivative ratio algorithm: Avoiding atmospheric effects in remote sensing," *IEEE Trans. Geosci. Remote Sens.* 29:250-357.

Ritchie, J.C., and C.M. Cooper, 1991, "An algorithm for estimation surface suspended sediment concentrations with Landsat MSS digital data," *Water Resources Bulletin*, 27(3): 373-379.

Ruiz-Azuara, P., 1995, “Multitemporal analysis of "simultaneous" Landsat imagery (MSS and TM) for monitoring primary production in a small tropical coastal lagoon,” *Photogrammetric Engineering & Remote Sensing*, 61(2):877-898.

Thomann, R.V. and Mueller, J.A., 1987, Principles of Surface Water: Quality Modeling and Control, Addison-Wesley Publishing Company: 694 pp., Facsimile edition (June, 1987).

Verdin, J.P., 1985, “Monitoring water quality conditions in a large western reservoir with Landsat imagery,” *Photogram. Eng. Rem. Sens*., 51, 343-353.

Wetzel, R. G., 1995, “Death, detritus and energy-flow in aquatic ecosystems.” *Freshwater Biology*, 33, 83-89.